

Non-thermal production of lepton asymmetry and dark matter in minimal seesaw with right handed neutrino induced Higgs potential

Rome Samanta,^{1, a} Anirban Biswas,^{2, b} and Sukannya Bhattacharya^{3, c}

¹*Physics and Astronomy, University of Southampton, Southampton, SO17 1BJ, U.K.*

²*School of Physical Sciences, Indian Association for the Cultivation of Science,
2A & 2B Raja S.C. Mullick Road, Kolkata 700032, India*

³*Theoretical Physics Division, Physical Research Laboratory,
Navrangpura, Ahmedabad-380009, India*

Within Type-I seesaw mechanism, Higgs mass can be dynamically generated via quantum effects of the right handed neutrinos assuming the potential is nearly conformal at the Ultra-Violet. The scenario, named as the “Neutrino Option” allows RH neutrino mass scale upto $M \lesssim 10^7$ GeV to be consistent with light neutrino masses, mixing and Higgs mass. Therefore, it is not consistent with standard hierarchical thermal leptogenesis. Parameter space for thermal resonant leptogenesis is highly constrained in this model. We point out that non-thermal pair production of RH neutrinos from inflaton decay corresponds in general to a mild degree of resonance in the CP asymmetry parameter and allows RH mass scale to be smaller more than by an order of magnitude than the thermal strong resonance case. Within the similar parameter space of thermal leptogenesis, RH neutrinos can also be produced from inflaton decay along with a Dark Matter having mass $M_{\text{DM}} \lesssim 320$ MeV. The main constraint in the latter scenario comes from the $L\gamma$ constraints on Dark Matter free streaming. We show in addition, that the Neutrino Option introduces a ‘phantom window’ for the RH mass scale, in which contrary to the usual scenarios, CP asymmetry parameter for leptogenesis decreases with the increase of the RH mass scale and minimally fine-tuned seesaw models naturally exhibit this ‘phantom window’.

^a romesamanta@gmail.com

^b anirban.biswas.sinp@gmail.com

^c sukannya@prl.res.in

I. INTRODUCTION

The fact that light neutrinos have mass is well established now, thanks to dedicated neutrino oscillation experiments[1–13]. The simplest and minimal theory which explains light neutrino masses beyond the Standard Model (SM) is the Type-I seesaw mechanism[14–16]. In this mechanism, minimum requirement of two heavy right handed (RH) neutrinos to generate light Majorana neutrino states also facilitates lepton number violating processes in the early universe which may be the underlying theory behind the observed dominance of matter over antimatter[17]. A lepton asymmetry (leptogenesis) which can further be converted into baryon asymmetry (baryogenesis) by $B - L$ - conserving sphaleron processes[18, 19] may originate from several sources, e.g., primordial gravitational waves[20–22], due to asymmetric propagation of leptons and anti-lepton in curved space time[23, 24], CP violating couplings between the Ricci scalar and fermions [25–28] etc.. However, in the context of particle physics, leptogenesis mechanisms involving RH neutrinos are widely studied since they are automatic consequences of the RH neutrino-extended theories of SM which also explain non-vanishing light neutrino masses. There are several variations of RH neutrino-induced leptogenesis mechanisms. Leptogenesis from RH neutrino decays[29–33], leptogenesis from RH neutrino oscillation[34] and a recently proposed mechanism of leptogenesis from Higgs decays[35]. In this work we stick to the simplest one, wherein CP violating and out of equilibrium decays of RH neutrinos create lepton asymmetry. It can be shown that if the RH neutrino masses are hierarchical, the minimum RH mass scale required for successful leptogenesis is $M_1 \gtrsim 10^9$ GeV- known as Davidson-Ibarra (DI) bound[36]. However, due to the RH neutrino involved Yukawa interactions, the *classical* Higgs potential suffers radiative corrections which monotonically increase with the increase of the RH masses. Not allowing the correction to the Higgs mass to exceed more than $\mathcal{O}(\text{TeV})$ -so called the naturalness problem[37–39], puts an upper bound on the RH mass scale $M \lesssim 10^7$ GeV which is well below the standard DI bound. Therefore, one needs to go beyond the hierarchical leptogenesis. One such mechanism is resonant-leptogenesis[30, 40, 41] where due to the presence of two strongly quasi-degenerate RH neutrinos, the CP asymmetry parameter responsible for leptogenesis gets resonantly enhanced and opens up possibilities for successful leptogenesis even at RH mass scale $\mathcal{O}(\text{TeV})$.

Recently, it has been proposed (the idea named as “Neutrino Option”) that the mentioned naturalness problem can be avoided if the Higgs mass itself is generated due to the radiative corrections induced by the RH neutrinos assuming the tree-level potential is nearly conformal at the Ultra-Violet (UV)[42, 43]. The RH neutrino masses which break the conformal symmetry can be dynamically generated[44] which then trigger the Electroweak symmetry breaking. However, to be consistent with the Higgs mass and the light neutrino masses, the maximum RH mass scale one can reach up to is again $M \lesssim 10^7$ GeV[45, 46] and thus one needs to consider leptogenesis due to quasi-degenerate heavy neutrinos. Interestingly, unlike the two RH neutrino seesaw model subjected to naturalness constraints, now one can not lower the mass scale up to TeV[47] to have successful leptogenesis. The parameter space is highly constrained, e.g., for normal light neutrino mass ordering one obtains $M \lesssim 1.2 \times 10^6$ GeV[45]. The primary restriction comes from the thermal production of the RH neutrinos through Yukawa coupling and consequently a washout of the produced lepton asymmetry. The strength of the washout increases with the decrease of the RH mass scale due to the conditions imposed by the Neutrino Option (NeO) and thus even with a strong resonant enhancement ($\Gamma_i \simeq \Delta M$ [30], where Γ_i is the decay width of the i th heavy neutrino and

$\Delta M = M_2 - M_1$) in the CP asymmetry parameter, one cannot lower the mass scale beyond $\sim 10^6$ GeV.

In this work, in search for a larger parameter space for leptogenesis within NeO, we consider an alternative production mechanism for the RH neutrinos. We first sacrifice the fact, that the RH neutrinos are produced via Yukawa coupling by assuming $T_{\text{RH}} < M_i$, where T_{RH} is the reheat temperature after inflation. Then we consider that RH neutrinos get produced non-thermally by inflaton decay which is a standard practice in the studies of non-thermal leptogenesis[48–56]. Once we have $T_{\text{RH}} < M_i$ ¹, the lepton asymmetry washout processes can be neglected[31, 32] because in that case the thermal bath does not have sufficient energy to reproduce RH neutrinos. Thus the final lepton asymmetry depends on the inflaton mass (m_ϕ), T_{RH} and the branching ratio for inflaton to RH neutrino decays. Without going into the details of a complete inflationary dynamics which includes the process of reheating, we consider instantaneous reheating[48, 53, 57] after inflation. We show that in the case of pair production of the RH neutrinos from inflaton decay, depending on the T_{RH} and inflaton mass, lower bounds on the RH mass scale can be relaxed by more than an order of magnitude than what is obtained in the thermal case. Allowed parameter space exhibits in general mild-resonant ($\Gamma_i \ll \Delta M$) solutions². Then we show that the non-thermal scenario also allows simultaneous production of RH neutrinos and Dark Matter (DM) almost within the same allowed range of RH neutrino masses, obtained in the case of successful thermal leptogenesis. The non-thermal DM produced through freeze-in is also another interesting proposal like non-thermal leptogenesis, explaining the null results in direct detection experiments naturally [58] and has been extensively studied in last few years [59–65]. In the present work, one of the important constraints comes from the Lyman- α forest data on DM free streaming ($\lambda_{FS} \lesssim 1$ Mpc, with λ_{FS} being the DM free-streaming length). This eventually puts a strong upper bound on branching ratio of inflaton decaying into RH neutrino and DM. To obtain the observed baryon asymmetry and at the same time reproducing correct DM relic density, we have found that the DM mass should always be less than 320 MeV. Finally, we point out that non-thermal leptogenesis when combined with NeO opens up a new window in the RH mass scale where contrary to usual scenarios, the CP asymmetry parameter required for leptogenesis, decreases with the increase of RH mass scale. We call this window as a “phantom window” (PW) and discuss importance of this PW in minimally fine tuned seesaw models. We do not present any explicit model and its possible conformal UV completion. We restrict ourselves only into the detailed study of thermal vs. non-thermal production of lepton asymmetry/dark matter within the NeO.

The rest of the paper is organised as follows. In Sec.II, we briefly discuss the framework of Neutrino Option. In Sec.III we discuss the inflaton decay to RH neutrinos and DM in a general context. Sec.IV contains a discussion of inflaton decay within the Neutrino Option. We summarise our results in Sec.V.

¹ In the numerical computation this condition has been implemented properly, using exact value of the temperature where the washout processes go out of equilibrium.

² Whenever we mention mild-resonant solutions, we always mean the departure ($\Gamma_i \ll \Delta M$) from the Pilaftsis-Underwood strong resonant condition $\Gamma_i \simeq \Delta M$ [30].

II. THE NEUTRINO OPTION

It is well known that in presence of the heavy RH neutrinos in the seesaw Lagrangian

$$-\mathcal{L}^{\text{seesaw}} = f_{\alpha i} \bar{\ell}_{L\alpha} \tilde{H} N_{Ri} + \frac{1}{2} \bar{N}_{Ri}^C (M_R)_{ij} \delta_{ij} N_{Rj} + \text{h.c.}, \quad (\text{II.1})$$

where $l_{L\alpha} = (\nu_{L\alpha} \ e_{L\alpha})^T$ is the SM lepton doublet of flavor α , $\tilde{H} = i\sigma^2 H^*$ with $H = (H^+ \ H^0)^T$ being the Higgs doublet and $M_R = \text{diag}(M_1, M_2, M_3)$, $M_{1,2,3} > 0$, the tree level Higgs potential

$$V_0 = -\frac{M_{H^0}^2}{2} H^\dagger H + \lambda_0 (H^\dagger H)^2 \quad (\text{II.2})$$

encounters large radiative correction (ΔM_H^2 and $\Delta\lambda$) which monotonically increases with the mass scale of the heavy neutrinos. In particular, for the sake of naturalness[38], the correction to Higgs mass not to exceed more than $\mathcal{O}(\text{TeV})$, one obtains an upper bound on the RH mass scale as $M \lesssim 10^7 \text{ GeV}$ [37]. The Neutrino Option[42, 43], a similar idea, however assumes the classical potential to be nearly conformal at the UV (here at the overall scale of the heavy RH neutrinos M), i.e.,

$$M_{H^0}(\mu > M) \simeq 0, \quad \lambda_0(\mu > M) \neq 0 \quad (\text{II.3})$$

with μ being the renormalization scale. The corrections are generated by the quantum effect of the RH neutrinos and hence break the invariance. Thus the values of M_H and λ at Electroweak (EW) scale can be extrapolated with RGEs upto the mass scale M to match the boundary conditions

$$M_H^2(\mu = M) \equiv \Delta M_H^2, \quad \lambda(\mu = M) \equiv \lambda_0 + \Delta\lambda, \quad (\text{II.4})$$

where in the limit of quasi-degenerate two heavy neutrinos, the radiative corrections ΔM_H^2 and $\Delta\lambda$ computed with dimensional regularisation within $\overline{\text{MS}}$ renormalisation scheme [42] reads

$$\Delta M_H^2(\mu = M) = \frac{1}{8\pi^2} \text{Tr} [f M^2 f^\dagger], \quad (\text{II.5})$$

$$\Delta\lambda(\mu = M) = -\frac{5}{32\pi^2} (|f_1|^4 + |f_2|^4 + 2 \text{Re}(f_1 \cdot f_2^*))^2 - \frac{1}{16\pi^2} \text{Im}(f_1 \cdot f_2^*)^2 \quad (\text{II.6})$$

with f_i as the i th column of the Yukawa matrix f . Barring any fine tuning within the Yukawa entries (discussed later), the threshold correction to the Higgs mass can be re-cast as

$$\Delta M_H^2(\mu = M) = \frac{M_i^3}{4\pi^2 v^2} \bar{m}, \quad (\text{II.7})$$

where \bar{m} is a overall mass scale of the light neutrinos and is given by $\bar{m} = \frac{|f_i|^2 v^2}{2M_i}$. For example, putting low energy neutrino data[13] and Higgs mass at EW scale, one obtains the RH mass scale $M \sim 10^7 \text{ GeV}$. Due to insignificant running of the Higgs mass as well as light neutrino masses through SM RGEs (assuming the heavy states are decoupled and we are left with only seesaw-EFT[66, 67]), the relation in Eq.II.7 works well at low energies. Within this region of the parameter space the correction to λ_0 can also be neglected[43]. Eq.II.7 (with a more accurate version discussed in Sec.IV) is the main constraint on the parameter space of leptogenesis in Neutrino Option.

III. THE MECHANISM

We first formulate the case of simultaneous non-thermal production of RH neutrinos and DM by considering a coupling [68–72]

$$\mathcal{L}^{N_i, DM} \sim y_\chi \bar{\chi} \phi N_i, \quad \text{with } i = 1, 2 \quad (\text{III.1})$$

where the field ϕ is the inflaton, N_i s are the two RH neutrinos and χ is a fermionic dark matter candidate. The case of pair production, i.e., $\phi \rightarrow N_i N_i$ will then be easy to understand and we shall mention it in relevant places alongside the present scenario. We assume that after the end of inflation the energy density ($n_\phi m_\phi = \rho_r = \pi^2 g_* T^4/30$) of inflaton field is transferred to the energy density of the radiation dominated universe. Thus the number densities of the RH neutrinos and Dark Matter are given by

$$N_{N_1} \equiv N_{N_2} = B_\chi g_{\text{eff}} \frac{\pi^4 T_{\text{RH}}}{30 m_\phi}, \quad N_{\text{DM}} = B_\chi g_{\text{eff}} \frac{\pi^4 T_{\text{RH}}}{15 m_\phi}, \quad (\text{III.2})$$

where $g_{\text{eff}} = g_*/g_{N_i}$ with g_* and g_{N_i} as the total relativistic degrees of freedom and spin degrees of the RH neutrinos respectively. In addition, we have assumed the branching ratios of $\phi \rightarrow N_i \chi$ decays are the same (i.e., $B_\chi^{N_1} \equiv B_\chi^{N_2} \sim B_\chi$, so that $n_{N_i, \text{DM}} \equiv B_\chi n_\phi$) and $N_{N_i, \text{DM}}$ are number densities normalised to the ultra-relativistic equilibrium number densities ($n_{i, \text{eq}}^{\text{ur}} = g_{N_i} T^3/\pi^2$) of N_i s. The Dark matter relic abundance³ is given by [73]

$$\Omega_{\text{DM}} h^2 = \frac{M_{\text{DM}} n_\gamma^0}{10.54 f(T_{\text{RH}}, T_0) \text{GeV m}^{-3}} \left(\frac{N_{\text{DM}}}{N_\gamma} \right)_{T_{\text{RH}}} \simeq 1.45 \times 10^6 \left(\frac{N_{\text{DM}}}{N_\gamma} \right)_{T_{\text{RH}}} \left(\frac{M_{\text{DM}}}{\text{GeV}} \right), \quad (\text{III.3})$$

where $n_\gamma^0 \simeq 410.7 \times 10^6 \text{m}^{-3}$ and $f(T_{\text{RH}}, T_0) \simeq 27.3$ are the relic photon number density at the present time and photon dilution factor respectively. When combined with the latest Planck satellite results [74] for $\Omega_{\text{DM}} h^2 \simeq 0.12$, from Eq. III.3 one finds

$$N_{N_{\text{DM}}} \simeq 1.1 \times 10^{-7} \left(\frac{\text{GeV}}{M_{\text{DM}}} \right). \quad (\text{III.4})$$

Now from the second equation of Eq. III.2 and Eq. III.4 one gets a generic expression for the reheating temperature T_{RH} as

$$T_{\text{RH}} \simeq \frac{15 \times 10^{-7}}{B_\chi g_{\text{eff}} \pi^4} \left(\frac{\text{GeV}}{M_{\text{DM}}} \right) m_\phi. \quad (\text{III.5})$$

The $B - L$ asymmetry is given by [31]

$$N_{B-L}^{\text{lepto}} = \sum_i^2 \varepsilon_i \kappa_i, \quad (\text{III.6})$$

where ε_i is the unflavoured CP asymmetry parameter corresponding to i th RH neutrino and κ_i is the efficiency of the asymmetry production with an explicit expression given by [31, 75]

$$\kappa_i(z = M_1/T) = - \int_{z_{\text{T}_{\text{RH}}}}^z \frac{dN_{N_i}}{dz'} e^{-\sum_i \int_{z'}^z W_i^{\text{ID+S}}(z'') dz''} dz', \quad (\text{III.7})$$

³ We are neglecting the annihilation cross sections of the processes like $N_i N_j \rightarrow \chi \chi$. Since our preferred value of T_{RH} is less than the RH neutrino masses, $\langle \sigma v \rangle_{N_i N_j \rightarrow \chi \chi}$ highly suppressed and hence after reheating, it cannot generate appreciable freeze in density of χ to account for. Details are given in appendix.

where $W_i^{\text{ID+S}}$ includes the inverse decay and scattering processes that tend to washout the lepton asymmetry[31, 32]. Since we are assuming non-thermal production of the asymmetry, i.e., $T_{\text{RH}} < M_i$, the washout effects ($W_i^{\text{ID+S}}$) are negligible. Thus the total lepton asymmetry is given by[31]

$$N_{B-L} = \sum_i N_{N_i} \Big|_{\text{RH}} \varepsilon_i \equiv \frac{\pi^4 B_X g_{\text{eff}}}{30} \sum_i \frac{\varepsilon_i T_{\text{RH}}}{m_\phi} \quad (\text{III.8})$$

with $N_{B-L}^{\text{Obs}} \simeq 6.1 \times 10^{-8}$ [17]. Combining Eq.III.5 and Eq.III.8 we obtain the master equation for the $B - L$ asymmetry as

$$N_{B-L} = N_{B-L}^{\text{Obs}} (\varepsilon_1 + \varepsilon_2) \left(\frac{\text{GeV}}{1.22 M_{\text{DM}}} \right) \equiv (\varepsilon_1 + \varepsilon_2) \kappa_{\text{Dark}}, \quad (\text{III.9})$$

where Eq.III.9 has been written in an analogous form as that of Eq.III.6, though the physical meaning for the efficiency factors (κ_i and κ_{Dark}) are entirely different.

Non-thermal Dark matter can have large velocity ($v_D(t)$) at the matter radiation equality unless the T_{RH} is very high so that $v_D(t)$ is red-shifted[50, 53, 76]. The large velocity might result into large co-moving free-streaming length (horizon) λ_{FS} which is constrained by the Ly- α cloud as $\lambda_{\text{FS}} \lesssim 1 \text{ Mpc}^4$. An explicit expression for λ_{FS} is given by

$$\lambda_{\text{FS}} \equiv \int_{t_{\text{RH}}}^{t_{\text{eq}}} \frac{v_D(t)}{a(t)} dt, \quad (\text{III.10})$$

where $a(t) \equiv a$ is the scale factor, t_{RH} and t_{eq} are times at the reheating and matter radiation equality respectively. With the velocity $v_D(t)$ is given as

$$v_D(t) \approx \frac{\frac{m_\phi a_{T_{\text{RH}}}}{2}}{\sqrt{M_{\text{DM}}^2 + \frac{m_\phi^2 a_{T_{\text{RH}}}^2}{4a(t)^2}}} \quad (\text{III.11})$$

and the Hubble expansion rate in the radiation domination⁵ $H \simeq H_0 \sqrt{\Omega_R^0} a^{-2}$ one simplifies Eq.III.10 as

$$\lambda_{\text{FS}} \simeq \frac{1}{H_0 \sqrt{\Omega_R^0}} \int_{a_{T_{\text{RH}}}}^{a_{\text{eq}}} \frac{da}{\sqrt{1 + X^2 a^2}}, \quad (\text{III.12})$$

where $X = \frac{2M_{\text{DM}}}{m_\phi a_{T_{\text{RH}}}}$. Integrating Eq.III.12 the free streaming length λ_{FS} can be obtained as

$$\lambda_{\text{FS}} \simeq \frac{\sqrt{\Omega_R^0}}{H_0 \Omega_M^0} P^{-1} \sinh^{-1} P, \quad (\text{III.13})$$

⁴ We use this value as a rough maximum allowed value of the free streaming length as considered in [53]. However, in realistic case, where one needs to compute the momentum distribution function of the DM as well as the transfer function (beyond the scope of this study) relating the matter power spectra of WDM and CDM scenarios[77], λ_{FS} might be smaller. Since this section we set up the general scenario we use $\lambda_{\text{FS}}^{\text{max}} \sim 1 \text{ Mpc}$. However, in section V where we discuss the Neutrino Option we shall use a realistic value of λ_{FS} [77] to constrain the parameter space.

⁵ The actual expression of H in the radiation dominated era is $H = H_0 \sqrt{\Omega_R^0} \left(\frac{g_*(T)}{g_*(T_0)} \right)^{1/3} a^{-2}$. Here we have neglected the ratio of energy degrees of freedom to get an analytical expression of λ_{FS} . This modifies λ_{FS} maximum by a factor of 3.

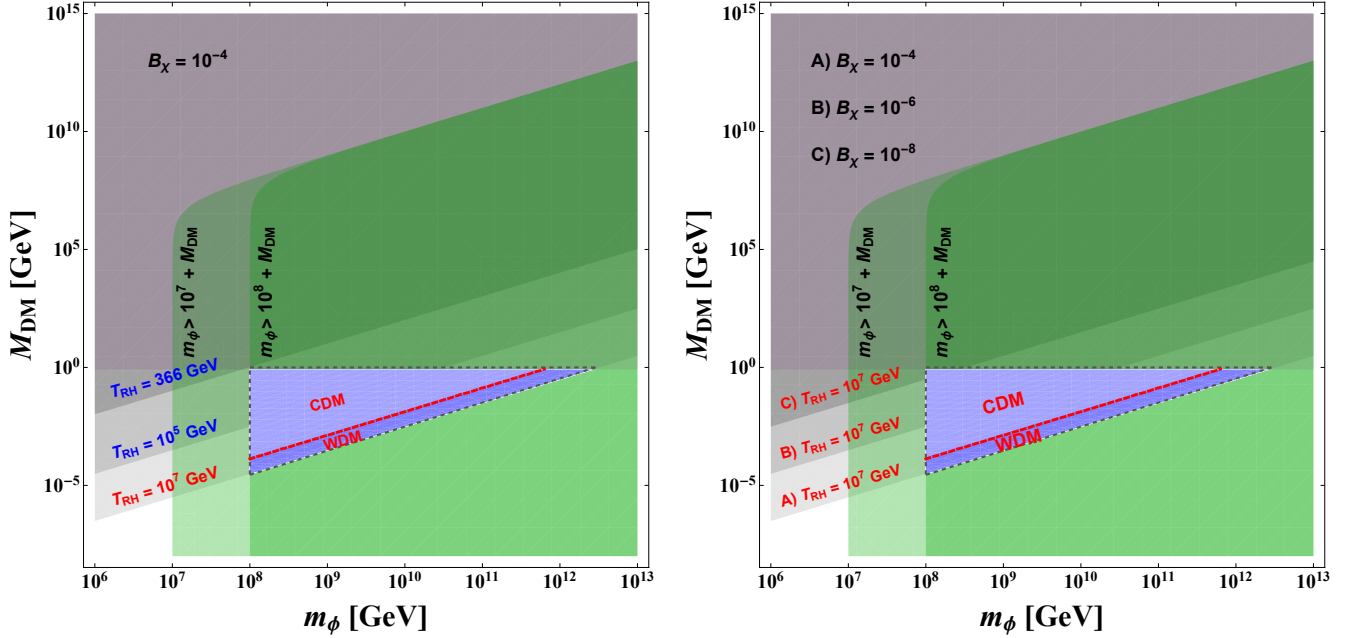


FIG. 1. Left: The green shades are the allowed region for the inflaton decay to be kinematically allowed, i. e. $m_\phi > M_{N_2} + M_{\text{DM}}$. We have shown two green regions for two benchmark values of M_{N_2} ($= 10^7$ GeV, 10^8 GeV). The pink shade from the top is the excluded region allowing $(\varepsilon_1 + \varepsilon_2)^{\text{max}} \approx 1$. The region bounded by the black dashed line is the maximum allowed region assuming $T_{\text{RH}}^{\text{max}} = 10^7$ GeV. The two purple shades separated by a red dashed line represent the CDM ($\lambda_{\text{FS}} \lesssim 10$ kpc [78, 79]) and WDM region corresponding to $T_{\text{RH}}^{\text{max}}$. Increasing gray gradients represent decrease in T_{RH} and hence truncation of the allowed parameter space. For $T_{\text{RH}} = 366$ GeV, the allowed parameter space closes which is consistent with Eq.III.20. It is evident that for $B_\chi = 10^{-4}$ and for $T_{\text{RH}} = 10^7$ GeV, correct relic density of DM is satisfied in the WDM region. Right: Except the gray gradients, all the color codes are the same as in the left panel. Increasing gray gradients represent decreasing branching fraction and allowed area of the parameter space. Notice that once B_χ decreases, correct relic density of DM is satisfied in the CDM region.

where $P = a_{\text{eq}}X$. Requiring $\lambda_{\text{FS}} \lesssim 1$ Mpc, with $H_0^{-1} \sim 4.422 \times 10^3$ Mpc and $\Omega_M^0 = 0.3147$ from Planck 2018 [74], $t_{\text{eq}} \sim 2 \times 10^{12}$ sec., and $t_{\text{RH}} \sim 1/\Gamma_\phi^{\text{tot}} \equiv (\pi^2 g_*/30)^{-1/2} M_P/T_{\text{RH}}^2$ one obtains a lower bound on the reheating temperature as

$$T_{\text{RH}} \gtrsim 3.56 \times 10^5 \text{ GeV} (g_*/200)^{-1/4} \left(\frac{\text{GeV}}{M_{\text{DM}}} \right) \left(\frac{m_\phi}{10^{12} \text{ GeV}} \right). \quad (\text{III.14})$$

When combined with Eq.III.5, the above translates in the upper bound on the branching ratio as

$$B_\chi \lesssim \frac{4.22}{\pi^4 g_{\text{eff}}} (g_*/200)^{1/4}. \quad (\text{III.15})$$

We can choose a representative value of $B_\chi = 10^{-4}$, which satisfies the above upper limit. However, the parameter space for the smaller values for B_χ has been shown in the right panel of Fig.1. One has also to take into account the constraints on the inflaton mass and the

benchmark value (for which we want to discuss the model parameter space) of the reheating temperature (T_{RH}^b) as

$$m_\phi^{\min} > M_i + M_{\text{DM}}, T_{\text{RH}}^b \lesssim M_i. \quad (\text{III.16})$$

The second constraint in Eq.III.16 when combined with Eq.III.5 translates into

$$\left(\frac{M_{\text{DM}}}{\text{GeV}}\right) \gtrsim \frac{3m_\phi}{10^4 \pi^4 T_{\text{RH}}^b}. \quad (\text{III.17})$$

Note that in Eq.III.17, we have used $B_\chi = 10^{-4}$. Finally, the maximum allowed value of the dark matter mass is given by Eq.III.9, i.e.,

$$\left(\frac{M_{\text{DM}}}{\text{GeV}}\right) \lesssim \frac{(\varepsilon_1 + \varepsilon_2)^{\max}}{1.22}. \quad (\text{III.18})$$

Thus from Eq.III.16, Eq.III.17 and Eq.III.18 it is clear that in the m_ϕ - M_{DM} plane, the shape of the allowed parameter space is a triangle with area given by

$$\frac{\mathcal{A}}{\text{GeV}^2} = \frac{1}{2} \left(\frac{(\varepsilon_1 + \varepsilon_2)}{1.22} - 0.03 \frac{m_\phi^{\min}}{10^4 T_{\text{RH}}^b} \right) \left(3.2 \times 10^6 \frac{(\varepsilon_1 + \varepsilon_2)}{1.22} T_{\text{RH}}^b - m_\phi^{\min} \right). \quad (\text{III.19})$$

From Eq.III.19, one obtains a lower bound on the T_{RH}^b as

$$T_{\text{RH}}^b \gtrsim \frac{0.0366 m_\phi^{\min}}{10^4 (\varepsilon_1 + \varepsilon_2)}. \quad (\text{III.20})$$

For example, in an extreme fine tuned condition of $(\varepsilon_1 + \varepsilon_2)^{\max} \approx 1$ and a benchmark value $m_\phi^{\min} \sim 10^8$ GeV one obtains the lower bound on the reheating temperature in this scenario⁶ as $T_{\text{RH}}^{\min} = 366$ GeV. In Fig.1 we show the maximum allowed parameter space for a minimum bench mark value of inflaton mass $m_\phi^{\min} = 10^8$ GeV. The red line of which separates the regions of Cold Dark Matter (CDM) and the Warm Dark Matter (WDM), corresponds the free streaming length $\lambda_{\text{FS}} = 10$ kpc, a value taken from Ref.[78, 79] which was also used in Ref.[53]. We would like to point out that while deriving lower bound on the reheat temperature with Eq.III.5, one has to be a bit more careful. This is since, in the left panel of Fig.1 we assume whatever be the choices of T_{RH} , the CP asymmetry parameter $\varepsilon_1 + \varepsilon_2$ remains constant. However, since the choice of T_{RH} depends on the RH masses and so is $\varepsilon_1 + \varepsilon_2$, one has to consider these two effect simultaneously. We properly consider this while extracting the parameter space for leptogenesis in Neutrino Option. Note that in the case of pair production $\phi \rightarrow N_i N_i$ for which RHS of Eq.III.8 will be enhanced by a factor 2, there is no such constraints on the branching ratio B_χ [54, 80]. Thus one expects larger parameter space in this case as we shall show in the next section. Having set up all the necessary prerequisites we now move to the discussion of non-thermal lepton asymmetry and DM production in the context of Neutrino Option.

⁶ The benchmark value $B_\chi = 10^{-4}$ can be slightly relaxed by demanding $T_{\text{RH}} \simeq T_{\text{Sph}}$ with T_{Sph} being the Sphaleron freeze out temperature. In that case, one obtains $B_\chi = \frac{0.03m_\phi}{T_{\text{Sph}} 10^8 (\varepsilon_1 + \varepsilon_2)^{\max}}$. Thus for our preferred set of values, B_χ can be relaxed to $B_\chi \sim 2 \times 10^{-4}$, where we use $T_{\text{Sph}} = 132$ GeV.

IV. THE SCENARIO OF $\phi \rightarrow N_i \chi, N_i N_i$ DECAYS WITHIN THE NEUTRINO OPTION

Starting from the neutrino part of the seesaw Lagrangian in Eq.II.1

$$-\mathcal{L}_{mass}^{\nu, N} = \bar{\nu}_{L\alpha}(m_D)_{i\alpha} N_{Ri} + \frac{1}{2} \bar{N}_{Ri}^C (M_R)_{ij} \delta_{ij} N_{Rj} + \text{h.c.}, \quad (\text{IV.1})$$

the effective light neutrino mass matrix can be obtained with the seesaw mechanism[14] as

$$M_\nu = -m_D M_R^{-1} m_D^T. \quad (\text{IV.2})$$

The mass matrix in Eq.IV.2 can be put into diagonal form by a unitary matrix U as

$$U^\dagger m_D M_R^{-1} m_D^T U^* = D_m \quad (\text{IV.3})$$

where $D_m = -\text{diag}(m_1, m_2, m_3)$ with $m_{1,2,3}$ being the physical light neutrino masses. We work in a basis where the charged lepton mass matrix m_ℓ and the RH neutrino mass matrix M_R are diagonal. Thus, the neutrino mixing matrix U can be written as

$$U = P_\phi U_{PMNS} \equiv P_\phi \begin{pmatrix} c_{12}c_{13} & e^{i\frac{\alpha}{2}} s_{12}c_{13} & s_{13}e^{-i(\delta-\frac{\beta}{2})} \\ -s_{12}c_{23} - c_{12}s_{23}s_{13}e^{i\delta} & e^{i\frac{\alpha}{2}}(c_{12}c_{23} - s_{12}s_{13}s_{23}e^{i\delta}) & c_{13}s_{23}e^{i\frac{\beta}{2}} \\ s_{12}s_{23} - c_{12}s_{13}c_{23}e^{i\delta} & e^{i\frac{\alpha}{2}}(-c_{12}s_{23} - s_{12}s_{13}c_{23}e^{i\delta}) & c_{13}c_{23}e^{i\frac{\beta}{2}} \end{pmatrix}, \quad (\text{IV.4})$$

where $P_\phi = \text{diag}(e^{i\phi_1}, e^{i\phi_2}, e^{i\phi_3})$ is an unphysical diagonal phase matrix and $c_{ij} \equiv \cos \theta_{ij}$, $s_{ij} \equiv \sin \theta_{ij}$ with the mixing angles $\theta_{ij} = [0, \pi/2]$. Low energy CP violation enters in Eq. IV.4 through the Dirac phase δ and the Majorana phases α and β . As an aside, it is convenient to parametrise (which can be straightforwardly derived from Eq.IV.3) the Dirac mass matrix as

$$m_D = U \sqrt{D_m} \Omega \sqrt{M_R}, \quad (\text{IV.5})$$

where Ω is a 3×3 complex orthogonal matrix that contains high energy CP phases. The parametrisation of the Dirac matrix, known as the Casas-Ibarra parametrisation[81] is an important and useful parametrisation particularly in the studies of leptogenesis, since depending upon the structure of the orthogonal matrix it becomes easier to understand whether leptogenesis is driven by the low energy or high energy CP phases. Before going into the detail discussion of leptogenesis in the scenario under consideration, in Table I, let's present the latest fact file for the light neutrinos.

TABLE I. Input values used in the analysis (inclusive of SK data)[13]

Parameter	θ_{12} degrees	θ_{23} degrees	θ_{13} degrees	Δm_{21}^2 $10^{-5}(\text{eV})^2$	$ \Delta m_{31}^2 $ $10^{-3}(\text{eV}^2)$
3σ ranges (NO)	31.61 – 36.27	41.1 – 51.3	8.22 – 8.98	6.79 – 8.01	2.44 – 2.62
3σ ranges (IO)	31.61 – 36.27	41.1 – 51.3	8.26 – 9.02	6.79 – 8.01	2.42 – 2.60
Best fit values (NO)	33.82	48.6	8.60	7.39	2.53
Best fit values (IO)	33.22	48.8	8.64	7.39	2.51

Compared to the previously released data[82], present best-fit value ($\sim 221^\circ$) for the Dirac CP violating phase (δ) exhibits a shift towards its CP conserving value for the Normal mass Ordering (NO), however for the Inverted mass Ordering (IO), best-fit of δ is still close to its maximal value ($\sim 282^\circ$). The Majorana phases remain unconstrained and there is preference of a NO over an IO.

Before the Electroweak Symmetry Breaking (ESB), the RH neutrinos decay to lepton doublets and Higgs (cf. Eq.II.1). In general, the produced lepton doublets $|\ell_i\rangle$ can be written as a coherent superposition of the corresponding flavour states $|\ell_\alpha\rangle$ as,

$$|\ell_i\rangle = \mathcal{A}_{i\alpha} |\ell_\alpha\rangle \quad (i = 1, 2; \alpha = e, \mu, \tau) \quad (\text{IV.6})$$

$$|\bar{\ell}_i\rangle = \bar{\mathcal{A}}_{i\alpha} |\bar{\ell}_\alpha\rangle \quad (i = 1, 2; \alpha = e, \mu, \tau), \quad (\text{IV.7})$$

where the tree level amplitudes are given by

$$\mathcal{A}_{i\alpha}^0 = \frac{(m_D)_{i\alpha}}{\sqrt{(m_D^\dagger m_D)_{ii}}} \quad \text{and} \quad \bar{\mathcal{A}}_{i\alpha}^0 = \frac{(m_D^*)_{i\alpha}}{\sqrt{(m_D^\dagger m_D)_{ii}}}. \quad (\text{IV.8})$$

However, the mass regime we are working in ($M_i \lesssim 10$ PeV), the charged lepton interactions are strong enough[83–86] to completely break the coherence of $|\ell_i\rangle$ states and thereby resolve each of the flavours. Thus one has to track the asymmetry in individual flavours. The asymmetry in the flavour α is given by

$$N_{\Delta_\alpha} = \sum_i^2 \varepsilon_{i\alpha} \kappa_{i\alpha} \quad (\text{IV.9})$$

with the efficiency factor

$$\kappa_{i\alpha}(z) = - \int_{z_{\text{in}}}^z \frac{dN_{N_i}}{dz'} e^{-\sum_j \int_{z'}^z P_{j\alpha}^0 W_j^{\text{ID}}(z'') dz''} dz', \quad (\text{IV.10})$$

where $P_{i\alpha}^0 = |\mathcal{A}_{i\alpha}^0|^2$. With this definition, the total N_{B-L} asymmetry is given by

$$N_{B-L} = \sum_\alpha N_{\Delta_\alpha}. \quad (\text{IV.11})$$

As mentioned earlier, since in our case the production is non-thermal, the wash-out of the asymmetry is negligible and thus the efficiency factor κ is basically independent of the flavour index ‘ α ’. Therefore the total Lepton asymmetry is

$$N_{B-L} = \sum_\alpha N_{\Delta_\alpha} \equiv \sum_i \kappa_i \sum_\alpha \varepsilon_{i\alpha} \simeq \sum_i N_{N_i} \Big|_{\text{RH}} \varepsilon_i. \quad (\text{IV.12})$$

The flavoured CP asymmetry parameter is given by[30]

$$\varepsilon_{i\alpha} = - \frac{1}{4\pi v^2 h_{ii}} \sum_{j \neq i} \left[\text{Im}\{h_{ij}(m_D^\dagger)_{i\alpha}(m_D)_{\alpha j}\} g(x_{ij}) - \frac{(1-x_{ij}) \text{Im}\{h_{ji}(m_D^\dagger)_{i\alpha}(m_D)_{\alpha j}\}}{(1-x_{ij})^2 + h_{jj}^2 (16\pi^2 v^4)^{-1}} \right], \quad (\text{IV.13})$$

where $h_{ij} = (m_D^\dagger m_D)_{ij}$, $x_{ij} = M_j^2/M_i^2$ and $g(x_{ij})$ is given by

$$g(x_{ij}) = \left[\sqrt{x_{ij}} \left[1 - (1 + x_{ij}) \ln \left(\frac{1 + x_{ij}}{x_{ij}} \right) \right] + \frac{\sqrt{x_{ij}}(1 - x_{ij})}{(1 - x_{ij})^2 + h_{jj}^2(16\pi^2 v^4)^{-1}} \right]. \quad (\text{IV.14})$$

Since h_{ij} is a hermitian matrix, when summed over α , the second term in Eq. IV.13 vanishes. Using the orthogonal parametrisation for m_D given in Eq. IV.5, the total CP asymmetry parameter (which is relevant in our case, cf. Eq. IV.12) can be written as

$$\begin{aligned} \varepsilon_i &= -\frac{1}{4\pi v^2} \sum_{\alpha} \frac{\text{Im}[M_j \sum_{kk'} \sqrt{m_k m_{k'}} m_k \Omega_{ki}^* \Omega_{k'i}^* U_{k'\alpha}^\dagger U_{\alpha k}] g(x_{ij})}{\sum_{k''} m_{k''} |\Omega_{k''i}|^2}, \\ &= -\frac{1}{4\pi v^2} \frac{M_j g(x_{ij}) \sum_k m_k^2 \text{Im}[\Omega_{ki}^* \Omega_{ki}]}{\sum_{k''} m_{k''} |\Omega_{k''i}|^2} \quad \text{with } i, j (i \neq j) = 1, 2. \end{aligned} \quad (\text{IV.15})$$

Note that the total CP asymmetry parameter given in Eq. IV.15 is independent of light neutrino mixing angles and low energy CP violating phases. Thus this scenario is insensitive in general to neutrino experiments. In addition, the models which predict a real or purely imaginary orthogonal matrix, see e.g., Refs. [87–93], can not generate baryon asymmetry via leptogenesis. Thus non-thermal leptogenesis scenario is not compatible with models of those kind. For simplicity, we shall work in a two RH neutrino scenario assuming the third one is heavier enough to be decoupled from the seesaw formula. In that case, the orthogonal matrices for NO ($m_1 = 0$) and IO ($m_3 = 0$) are given by

$$\Omega^{\text{NO}} = \begin{pmatrix} 0 & 0 & 1 \\ \cos \theta & \sin \theta & 0 \\ -\sin \theta & \cos \theta & 0 \end{pmatrix}, \quad \Omega^{\text{IO}} = \begin{pmatrix} \cos \theta & \sin \theta & 0 \\ -\sin \theta & \cos \theta & 0 \\ 0 & 0 & 1 \end{pmatrix}, \quad (\text{IV.16})$$

where $\theta = x - iy$ is a complex angle with x and y being real parameters. Using Eq. IV.16 and maximising Eq. IV.15 with respect to x we get⁷

$$\varepsilon_1^{\text{NO}} = -\frac{M_2 g(x_{12})}{4\pi v^2} (m_3 - m_2) \tanh 2y, \quad (\text{IV.17})$$

$$\varepsilon_2^{\text{NO}} = \frac{M_1 g(x_{21})}{4\pi v^2} (m_3 - m_2) \tanh 2y \quad (\text{IV.18})$$

and

$$\varepsilon_1^{\text{IO}} = -\frac{M_2 g(x_{12})}{4\pi v^2} (m_2 - m_1) \tanh 2y, \quad (\text{IV.19})$$

$$\varepsilon_2^{\text{IO}} = \frac{M_1 g(x_{21})}{4\pi v^2} (m_2 - m_1) \tanh 2y. \quad (\text{IV.20})$$

From Eq. II.5, the threshold correction to the Higgs mass ΔM_H^2 can be written as

$$\Delta M_H^2 = \frac{1}{8\pi^2 v^2} \sum_i M_i^3 \sum_k m_k |\Omega_{ki}|^2 = \frac{m^*}{8\pi^2 v^2} \sum_i M_i^3 K_i \quad (\text{IV.21})$$

⁷ Since our aim is to extract maximum parameter space, we maximize the CP asymmetry parameter by putting $x = \pi/4$.

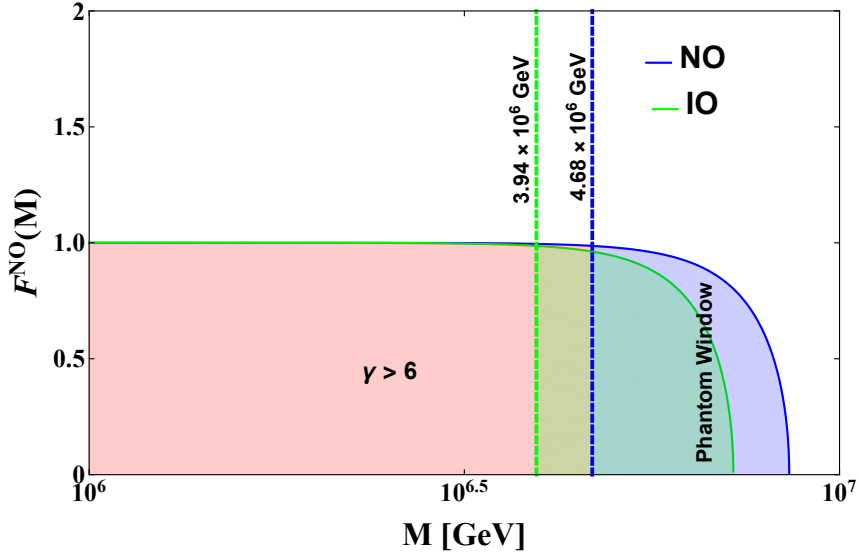


FIG. 2. Variation of the phantom function with the RH mass scale M . The green (for inverted ordering) and blue (for normal ordering) lines represent starting point of the phantom window which causes a decrease of the CP asymmetry parameter as the RH mass scale increases. The pink region belongs to boosted seesaw systems in which the phantom function saturates to 1.

where, the decay parameter for the i^{th} RH neutrino is defined as $K_i = \frac{\sum_k m_k |\Omega_{ki}|^2}{m^*}$ and m^* is the equilibrium neutrino mass given by $m^* \sim 10^{-3}$ eV[32]. The above expression in the quasi degenerate limit of the RH neutrino masses ($M_1 \simeq M_2 \simeq M$) simplifies to

$$\Delta M_H^{2\text{NO}} \simeq \frac{M^3}{8\pi^2 v^2} (m_3 + m_2) \cosh 2y, \quad \Delta M_H^{2\text{IO}} \simeq \frac{M^3}{8\pi^2 v^2} (m_2 + m_1) \cosh 2y. \quad (\text{IV.22})$$

Thus using Eq.IV.22 and Eq.IV.17-Eq.IV.20, the total CP asymmetry parameters can be simplified as

$$(\varepsilon_1 + \varepsilon_2)^{\text{NO}} = -\frac{m_3 - m_2}{4\pi v^2} [g(x_{12})M_2 - g(x_{21})M_1] F^{\text{NO}}(M_H, M, \sum_i m_i), \quad (\text{IV.23})$$

$$(\varepsilon_1 + \varepsilon_2)^{\text{IO}} = -\frac{m_2 - m_1}{4\pi v^2} [g(x_{12})M_2 - g(x_{21})M_1] F^{\text{IO}}(M_H, M, \sum_i m_i), \quad (\text{IV.24})$$

where

$$F^{\text{NO}}(M_H, M, \sum_i m_i) = \sqrt{1 - \left[\frac{M^3(m_3 + m_2)}{\Delta M_H^2 8\pi^2 v^2} \right]^2}, \quad (\text{IV.25})$$

$$F^{\text{IO}}(M_H, M, \sum_i m_i) = \sqrt{1 - \left[\frac{M^3(m_2 + m_1)}{\Delta M_H^2 8\pi^2 v^2} \right]^2}. \quad (\text{IV.26})$$

The function $F^{(\text{N,IO})}$, we call it a phantom function, renders a window to the RH mass scale (cf. Fig.2) in which it drives the CP asymmetry parameters to decrease with the increase of the RH mass scale. Furthermore, ε_i vanishes at M_{max} which can be calculated for $y = 0$ in

Eq. IV.22 for the respective ordering of light neutrino masses as $M_{\max}^{\text{NO}} \simeq 8.57 \times 10^6$ GeV and $M_{\max}^{\text{IO}} \simeq 7.21 \times 10^6$ GeV. Thus as the RH mass scale increases, in this window, one needs the RH neutrinos to be more quasi-degenerate to resonantly amplify the CP asymmetry parameter. This is a completely new behaviour of the CP asymmetry parameter introduced by the Neutrino Option. To stress more on the significance of the phantom window (PW) in seesaw models, let's have a brief look at the properties of the orthogonal matrix Ω . First of all, the quantity

$$\gamma_i = \sum_j |\Omega_{ij}^2| \geq 1 \quad (\text{IV.27})$$

accounts for the fractional contribution of the heavy M_j states to a particular light neutrino m_i , thus can be treated as a measure of fine-tuning in the seesaw formula[94]. In addition, since Ω belongs to $SO(3, \mathbb{C})$, it is isomorphic to the Lorentz group. Thus Ω can be factorized as

$$\Omega = \Omega^{\text{rotation}} \Omega^{\text{Boost}}. \quad (\text{IV.28})$$

Using Eq. IV.5 and Eq. IV.8 it is trivial to derive a transformation relation between the states produced by the RH neutrinos ($|\ell_j\rangle$) and the light neutrinos states ($|\tilde{\ell}_i\rangle$) as

$$|\ell_j\rangle = B_{ji} |\tilde{\ell}_i\rangle, \quad (\text{IV.29})$$

where the bridging matrix B_{ij} , first introduced in Ref.[94] relates the heavy and the light states with a non-orthonormal transformation (in general) and is related to the orthogonal matrix as

$$B_{ji} = \frac{\sqrt{m_i} \Omega_{ji}}{\sqrt{m_k |\Omega_{kj}|^2}}. \quad (\text{IV.30})$$

For a simple choice of the orthogonal matrix Ω which does not corresponds to any fine-tuning (a particular heavy neutrino contributes to a particular light neutrino[95]), e.g.,

$$\Omega^{\text{NO}} = \begin{pmatrix} 0 & 0 & 1 \\ 1 & 0 & 0 \\ 0 & 1 & 0 \end{pmatrix}, \quad (\text{IV.31})$$

the heavy and the light states coincide as shown in Fig.3. However this is not true in general. For the orthogonal matrix (cf. Eq. IV.16) which can be factorised as

$$\Omega^{\text{NO}} = \begin{pmatrix} 0 & 0 & 1 \\ \cos x & \sin x & 0 \\ -\sin x & \cos x & 0 \end{pmatrix} \begin{pmatrix} \cosh y & -i \sinh y & 0 \\ i \sinh y & \cosh y & 0 \\ 0 & 0 & 1 \end{pmatrix}, \quad (\text{IV.32})$$

the orthonormality in the heavy states does not hold unless one assumes $x, y = 0$. Specifically, due to the presence of the boost matrix, the heavy states are in general strongly non-orthonormal. Using Eq. IV.27 the fine-tuning parameters can be calculated as

$$\gamma_2 = \gamma_3 = \cosh 2y. \quad (\text{IV.33})$$

This explicitly shows how the boosted seesaw systems with strongly non-orthonormal heavy states may involve large amount of fine-tuning and the philosophy, that the separation

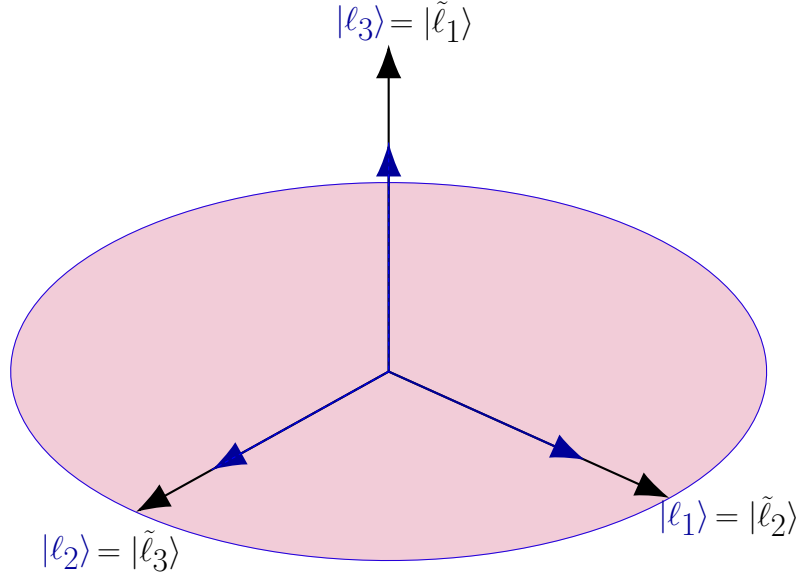


FIG. 3. Illustration of seesaw models with no fine tuning leading to vanishing lepton asymmetry. The state vectors in blue are heavy states produced by the RH neutrinos while the states in black correspond to the light neutrinos.

between two mass scales M and M_H (cf. Eq.IV.22) may be related to another experimentally observed light mass scale m_i , gets spoiled. From now on we call the ‘ γ_i ’ parameters as the boost parameters and the seesaw systems which correspond to $\gamma_i \approx 1$ as the minimally fine-tuned seesaw models or unboosted seesaw systems. In Fig.2, we show the variation of the phantom function $F^{(N,I)O}$ with the RH mass scale M . For the best fit values of the light neutrino masses given in Table I, we find

$$M_F^{\text{NO}} = 4.68 \times 10^6 \text{GeV}, \quad M_F^{\text{IO}} = 3.94 \times 10^6 \text{GeV}, \quad (\text{IV.34})$$

below which the function $F^{(N,I)O}$ saturates approximately to 1. Thus M_F^{NO} and M_F^{IO} can be regarded as the starting point of PW. Using Eq.IV.22, one finds, $M \lesssim M_F^{(N,I)O}$ corresponds to $\gamma_i \gtrsim 6$ which shows even the starting point of the PW corresponds to large fine-tuning in the seesaw formula.

Now we turn to the detail analysis of the model parameter space which satisfies correct DM relic density as well as observed baryon asymmetry (for the $\phi \rightarrow N_i \chi$ decay). First of all, the regulator term in Eq.IV.13 can be written as

$$\tilde{\Gamma}_2 = h_{22}/4\pi v^2 \simeq 1/4\pi v^2 \sum_k m_k |\Omega_{k2}|^2 M_2 \equiv \frac{m^*}{4\pi v^2} K_2 M_2 \simeq \tilde{\Gamma}_1. \quad (\text{IV.35})$$

With $\delta_{\text{lep}} = (M_2 - M_1)/M_1$, we define ratios

$$R^{\text{NO}} = \frac{\delta_{\text{lep}}}{\tilde{\Gamma}_2^{\text{NO}}}, \quad R^{\text{IO}} = \frac{\delta_{\text{lep}}}{\tilde{\Gamma}_2^{\text{IO}}} \quad (\text{IV.36})$$

which measure the departure from a pure Pilaftsis-Underwood resonance ($R^{(N,I)O} \sim 1$)[30]. Now using Eq.IV.24, the total CP asymmetry parameters in the quasi-degenerate limit of

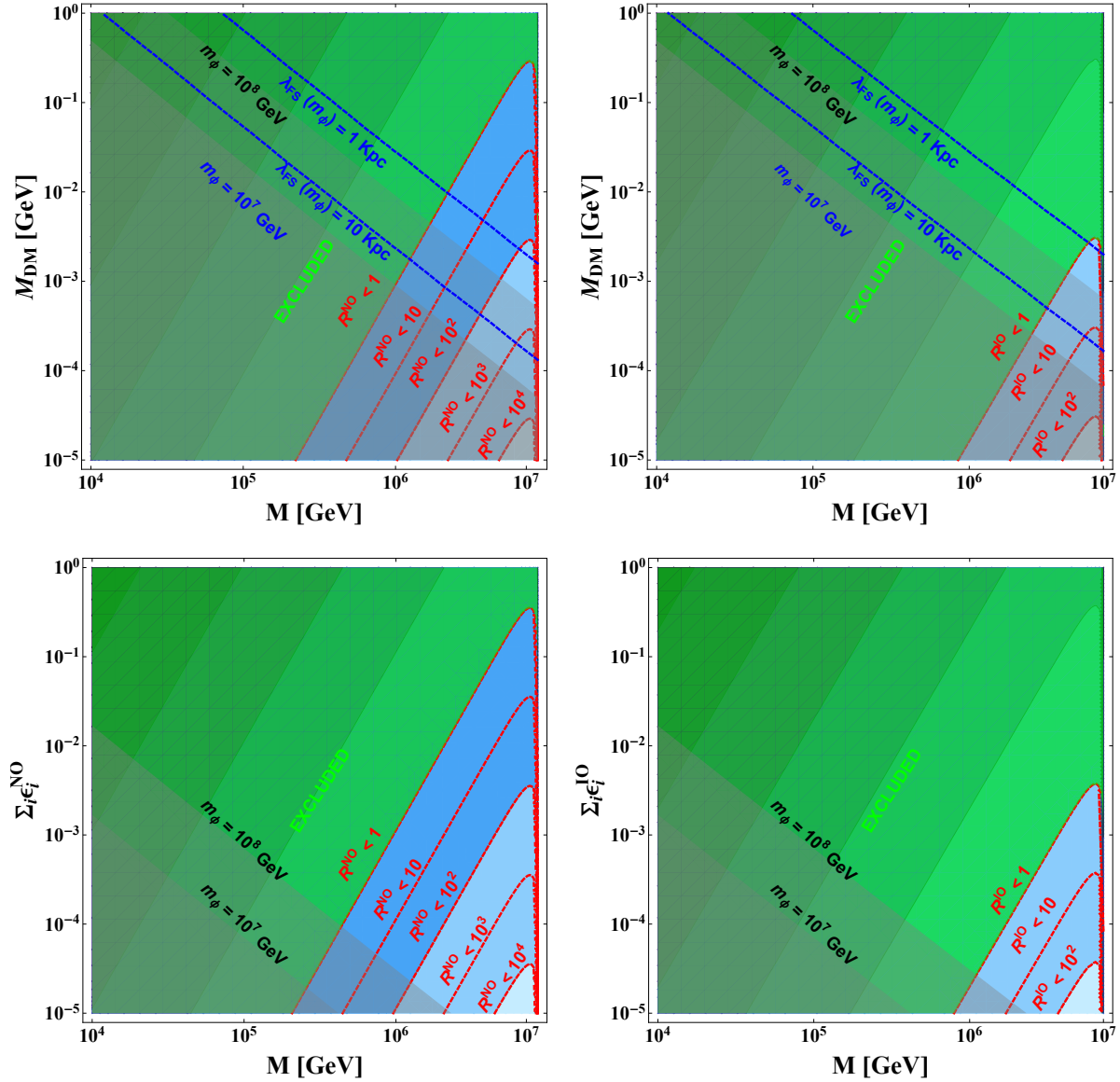


FIG. 4. In the $M - M_{\text{DM}}$ plane, allowed values of the R parameter which measures the departure from Pilaftsis-Underwood resonance for normal ordering (left) for inverted ordering (right). The green region is excluded as it corresponds to a value $R < 1$.

the RH masses can be written as

$$(\varepsilon_1 + \varepsilon_2)^{\text{NO}} = \frac{(m_3 - m_2)M}{8\pi v^2 \delta_{\text{lep}}^{\text{NO}}} \sqrt{1 - \left[\frac{M^3(m_3 + m_2)}{\Delta M_H^2 8\pi^2 v^2} \right]^2}, \quad (\text{IV.37})$$

$$(\varepsilon_1 + \varepsilon_2)^{\text{IO}} = \frac{(m_2 - m_1)M}{8\pi v^2 \delta_{\text{lep}}^{\text{IO}}} \sqrt{1 - \left[\frac{M^3(m_2 + m_1)}{\Delta M_H^2 8\pi^2 v^2} \right]^2}, \quad (\text{IV.38})$$

where M is the overall mass scale of the RH neutrinos and we ignore the regulator term in the CP asymmetry parameters. Using the master formula presented in Eq.III.9, it is now easy to find the values of the $R^{(\text{N,I})\text{O}}$ which satisfy correct baryon asymmetry and

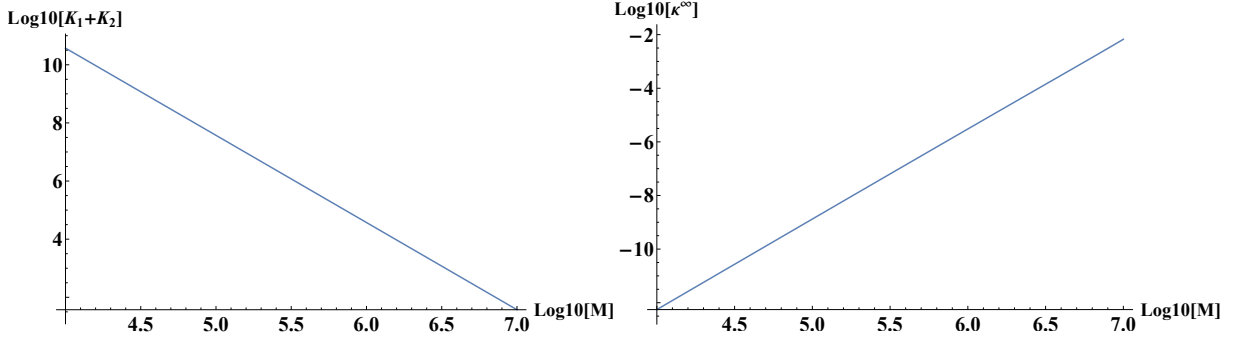


FIG. 5. Left: Variation of the sum of the decay parameters (which is responsible for washout of thermally generated lepton asymmetry) with the RH mass scale M . The nature of this variation is completely due to the conditions imposed by Neutrino Option. Right: variation of the efficiency factor κ^∞ with M .

correct DM relic density. In the upper panel of Fig.4, we show the allowed values of the R parameters in $M - M_{\text{DM}}$ plane. The green region in each plot corresponds to a super degenerate case ($R^{(\text{N,I})\text{O}} < 1$) [96] which we do not study in this paper. The gray shades are ruled out due the similar constraint derived in Eq.III.17 with the maximum branching ratio corresponding to free streaming half mode $k_{\text{FS}}^{1/2} \sim 40\text{h/Mpc}$ [77] for $m_\phi = 10^7$ GeV and $m_\phi = 10^8$ GeV respectively – we take the former value of m_ϕ to be the minimum one so that we can cover the maximum parameter space, i.e., $m_\phi > M_{\text{max}}^{(\text{N,I})\text{O}} + M_{\text{DM}}$. As mentioned earlier in the introduction, to draw the gray shaded region we use a more accurate value of the reheat temperature by generalising the condition $M_i > T_{\text{RH}}$ to $M_i > \Phi(K_i)T_{\text{RH}}$, where the function $\Phi(K_i)$ determines the value of $z_f = M/T$ after which washout processes go out of equilibrium. An explicit expression of the function can be calculated analytically[31] and for quasi degenerate heavy neutrinos it is given by

$$\Phi\left(\sum_i K_i\right) = 2 + 4\left(\sum_i K_i\right)^{0.13} + e^{\frac{-2.5}{\sum_i K_i}}, \quad (\text{IV.39})$$

where from Eq.IV.21, $\sum_i K_i$ can be expressed as a function of the Higgs and the RH neutrino masses as

$$K_1 + K_2 = \frac{8\Delta M_H^2 \pi^2 v^2}{m^* M^3}. \quad (\text{IV.40})$$

The blue dotted lines correspond to the free streaming lengths $\lambda_{\text{FS}} \simeq 10$ kpc and $\lambda_{\text{FS}} \simeq 1$ kpc for $m_\phi = 10^7$ GeV, where the former separates the CDM and WDM regions[78, 79] and we draw the latter to indicate that λ_{FS} decreases as DM mass increases – indicating a CDM region. Note that in both the plots, there exists a small range of the RH mass scale (from the point where the $\lambda_{\text{FS}} = 10$ kpc curve and $R^{(\text{N,I})\text{O}} = 1$ intersect to the point where curves correspond to $m_\phi = 10^7$ GeV and $R^{(\text{N,I})\text{O}} = 1$ intersect) in which the parameter space favours only WDM. We would also like to mention that the lower bounds on the RH masses we obtain in this case ($M^{\text{NO}} > 1.1 \times 10^6$ GeV and $M^{\text{IO}} > 2.6 \times 10^6$) are more or less similar to those obtained in the thermal case ($M^{\text{NO}} > 1.2 \times 10^6$ GeV and $M^{\text{IO}} > 2.4 \times 10^6$)[45]. It is evident that for NO, there is a large parameter space which allows mild-resonant solutions ($R^{\text{NO}} \gg 1$). However, for IO, the allowed parameter space gets reduced. This is since,

compared to the NO, CP asymmetry parameter is suppressed by the pre-factor $m_2 - m_1$ (cf. Eq.IV.38) in case of IO. Now we turn to case of pair production, i.e., $\phi \rightarrow N_i N_i$. In the lower panel, we show the allowed parameter space in the $\sum_i \varepsilon_i - M$ plane. The gray shades are due to the constraints derived from Eq.III.8 and it reads

$$\varepsilon_1 + \varepsilon_2 \geq N_{B-L}^{\text{Obs}} \left(\frac{15m_\phi}{\pi^4 B_\chi g_{\text{eff}}} \right) \frac{\Phi(\sum_i K_i)}{M}. \quad (\text{IV.41})$$

Taking $B_\chi \sim 10^{-2}$, compare to the thermal leptogenesis, we get more relaxed lower bounds on the RH masses for both the ordering of light neutrino masses as

$$M^{\text{NO}} \gtrsim 2.6 \times 10^5 \text{GeV}, \quad M^{\text{IO}} \gtrsim 6 \times 10^5 \text{GeV}. \quad (\text{IV.42})$$

Consequently the upper bounds on the reheat temperature come out as

$$T_{\text{RH}}^{\text{NO}} \leq 9.1 \times 10^3 \text{GeV}, \quad T_{\text{RH}}^{\text{IO}} \leq 2.8 \times 10^4 \text{GeV}. \quad (\text{IV.43})$$

Note that for NO, the lower bound is almost an order of magnitude below what is obtained in the thermal case. These bounds can be even more relaxed for larger values of B_χ [54, 80].

One might wonder why the mild-resonant solutions appear in our case, while for the thermal production of right-handed neutrinos, its clearly resonant even if the RH mass scale is $\sim 10^6$ GeV, as confirmed by Ref.[45]. The basic physical reason is, in the thermal case, Neutrino Option introduces a rapid exponential reduction of production efficiency with the decrease of RH mass scale. This can be seen by calculating the efficiency factor, say e.g.,

$$\kappa_i(z = M_1/T) = - \int_{z_{\text{T}_{\text{RH}}}}^z \frac{dN_{N_i}}{dz'} e^{-\sum_i \int_{z'}^z W_i^{\text{ID}}(z'') dz''} dz', \quad (\text{IV.44})$$

where we include only inverse decays at the washout for simplicity. After properly subtracting the real intermediate state contribution of $\Delta L = 2$ process[30, 97], W^{ID} can be written as

$$W_i^{\text{ID}} = \frac{1}{4} K_i (1 + \delta_{\text{lep}}) \mathcal{K}_1(z_i) z_i^3, \quad (\text{IV.45})$$

where $z_i = z(1 + \delta_{\text{lep}})$ and $\mathcal{K}_1(z_i)$ is modified Bessel function. Clearly, in the limit $\delta_{\text{lep}} \ll 1$, the total washout due to both the RH neutrinos can be approximated as

$$W_{\text{tot}}^{\text{ID}} \simeq \frac{1}{4} (K_1 + K_2) \mathcal{K}_1(z) z^3. \quad (\text{IV.46})$$

Thus in the quasi-degenerate limit of the RH neutrinos, the decay parameters (K_i) leave an additive contribution to the exponential washout. Eq.IV.40 justifies why even with a small decrease in M , the sum of the decay parameter rapidly increases (cf. Fig.5) and strongly washes out the produced lepton asymmetry. Thus one needs a resonant enhancement in the CP asymmetry parameter to compensate this strong washout. In the strong washout regime, the Yukawas will quickly thermalise the heavy neutrinos and the final asymmetry which is independent of initial conditions can be written as

$$N_{B-L}^{\text{Thermal}} = (\varepsilon_1 + \varepsilon_2) \kappa^\infty, \quad (\text{IV.47})$$

where κ^∞ is given by[31, 75]

$$\kappa^\infty = \frac{2}{\sum_i K_i \Phi(\sum_i K_i)} (1 - e^{-\frac{\sum_i K_i \Phi(\sum_i K_i)}{2}}). \quad (\text{IV.48})$$

In the right panel of Fig.5, we plot the efficiency factor with the mass scale M . Notice that around $M \sim 1.2 \times 10^6$ GeV, $\kappa^\infty \sim 6 \times 10^{-6}$ which requires $\varepsilon_1 + \varepsilon_2 \sim 10^{-2}$ to be consistent with N_{B-L}^{Obs} . Now going back to the bottom left panel of Fig.4, apparently, it seems that for $M \sim 1.2 \times 10^6$ GeV, the value of $\varepsilon_1 + \varepsilon_2 \sim 10^{-2}$ is outside the parameter space (i.e., the value is in the green region). However, recall that in thermal leptogenesis flavour effects which reduces the strength of the washout and increases the production efficiency[83–86], plays an important role and thus one can have the required CP asymmetry within the allowed parameter space. In any case, the rough estimate presented above clearly shows why around $M \sim 10^6$ GeV, the CP asymmetry parameter tends to hit $R \sim 1$ contour (resonant solution) for thermal leptogenesis. On the other hand, as already mentioned, for $\phi \rightarrow N_i \chi$ decays, we obtain approximately similar (what is obtained for thermal leptogenesis) allowed range for the RH neutrinos masses. Thus around $M \sim 10^6$ one should get $R \sim 1$ solutions which is exactly the case as shown in the upper left panel of Fig.5. In this case, though the efficiency factor

$$\kappa_{\text{Dark}} = N_{B-L}^{\text{Obs}} \left(\frac{\text{GeV}}{1.22 M_{\text{DM}}} \right) \quad (\text{IV.49})$$

is not constrained by the Neutrino Option, Eq.III.17 with $M_i > \Phi(K_i) T_{\text{RH}}$ for which we draw the blue and the gray shades, is affected by the Neutrino Option.

We conclude with the following remarks:

I) Since we have discussed quasi-degenerate RH mass spectrum and hence a single scale seesaw EFT[66, 67], we do not expect significant affect of RG group evolution on the derived parameter space.

II) Fig. 1 shows that the typical range of m_ϕ in such a process is $10^8 - 10^{12}$ GeV, which is in contradiction with the observational constraints on simple single field models of inflation. As an example, the mass of the inflaton in a chaotic quadratic inflation with $m_\phi^2 \phi^2$ potential is constrained from the precisely measured amplitude of the primordial scalar power spectrum in Planck 2018 [99] to be $m_\phi \sim 10^{13}$ GeV. However, multi-field models of inflation where the mass of the inflaton does not determine cosmological observables in Planck, can accommodate such values of m_ϕ as required in the DM and neutrino productions in this context. For example, hybrid inflation models [100, 101] can be good candidates for this case where the waterfall criteria are satisfied by tuning the mass and couplings of the waterfall field accordingly. However, when one analyses particular inflation models conforming with such a scenario, the bounds on the reheating temperature are also to be considered accordingly since the resulting parameter ranges for M_{DM} and M depend on T_{RH} . We have neglected also, e.g., possible impact of the strong Higgs-inflaton coupling which might put additional constraints on the parameter space. In any case, NeO itself requires a non-trivial conformal UV theory and so is the present scenario. The purpose of the entire study was to emphasise the difference between thermal and non-thermal production of lepton asymmetry using the constraints that come out of the NeO.

III) The lower bounds on M in Eq.IV.53 are obtained for $\Delta M \simeq \Gamma_i$. In this regime, there could be another contribution to the CP asymmetry parameter due the RH neutrino

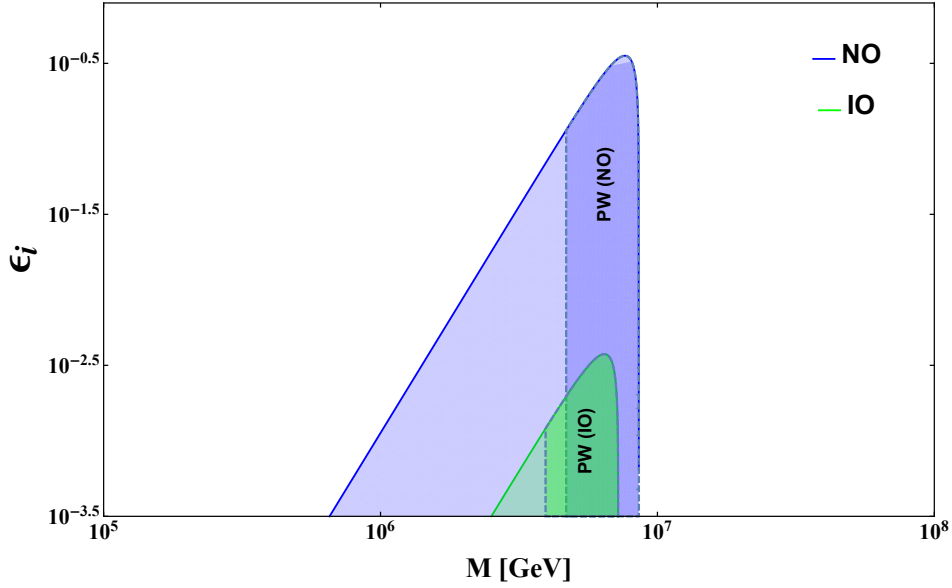


FIG. 6. Variation of the total CP asymmetry parameter with the RH mass scale M allowing Pilaftsis-Underwood resonance. The parameter space plotted in purple (green) is for normal mass ordering (inverted mass ordering). Maximum enhancement in the CP asymmetry parameter occurs at $M_{\max} = 7.63 \times 10^6$ GeV ($M_{\max} = 6.43 \times 10^6$ GeV) for normal mass ordering (inverted mass ordering).

oscillation in the thermal bath[40, 41]. In this case the loop function $g(x_{ij})$ in Eq.IV.13 can be replaced with

$$g(x_{ij})^{\text{tot}} \equiv g(x_{ij})^{\text{mix}} + g(x_{ij})^{\text{osc}}, \quad (\text{IV.50})$$

where $g(x_{ij})^{\text{mix}}$ is the usual loop function given in Eq.IV.14 and $g(x_{ij})^{\text{osc}}$ is given by

$$g(x_{ij})^{\text{osc}} = \frac{(1 - x_{ij})\sqrt{x_{ij}}}{(1 - x_{ij})^2 + M_i^{-2}(\Gamma_i + \sqrt{x_{ij}}\Gamma_j)^2 \frac{\det[\text{Re}(f^\dagger f)]}{(f^\dagger f)_{ii}(f^\dagger f)_{jj}}}. \quad (\text{IV.51})$$

When the effect of $g(x_{ij})^{\text{osc}}$ is taken into account, the lower bounds on M relax to

$$M^{\text{NO}} \gtrsim 2.1 \times 10^5 \text{GeV}, \quad M^{\text{IO}} \gtrsim 5.3 \times 10^5 \text{GeV}. \quad (\text{IV.52})$$

IV) For a particular value of x in the orthogonal matrix, there is a global maximum in the CP asymmetry parameter. In Fig.6, we show a representative parameter space in the $\varepsilon_i - M$ plane. Thus there is a distinct heavy RH scale for leptogenesis which can be found by obtaining the value of M at ε_{\max} . Maximizing the CP asymmetry parameter w.r.t x , we calculate them to be

$$M^{\text{NO}} \simeq 7.63 \times 10^6 \text{GeV}, \quad M^{\text{IO}} \simeq 6.43 \times 10^6 \text{GeV}. \quad (\text{IV.53})$$

Otherwise, there is always a pair of M for obtaining ε_i of same magnitude (see Fig.6). Note that, this typical feature of ε_i is driven by the newly introduced the phantom window which is a consequence of the consistency relation derived in Eq.IV.22. To distinguish such a mass degeneracy one needs to dig the dynamical origin of the RH masses in a UV theory[98] and study its signatures such as Gravitational wave which we shall consider in a future work.

V. SUMMARY

We discuss a non-thermal production mechanism of RH neutrinos and Dark Matter within the framework of Neutrino Option. Using the Type-I seesaw Lagrangian, the Neutrino Option—a mechanism of generating Higgs mass by the quantum effects of the RH neutrinos, puts an upper bound on the RH mass scale as $M \lesssim 10^7$ GeV and thereby does not facilitate hierarchical thermal leptogenesis. The parameter space for thermal resonant leptogenesis ($\Delta M \sim \Gamma_i$) is highly constrained due an increasing strong washout of the produced asymmetry with the decrease of the RH mass scale. In this article, we show that non-thermal pair production of the RH neutrinos from inflaton decay allows the RH mass scale to be smaller by more than an order of magnitude than what is obtained for the thermal case. Specially for normal light neutrino mass ordering, which is now favoured by oscillation experiments, the parameter space is in general mildly resonant ($\Delta M \gg \Gamma_i$). Then we show that the scenario of simultaneous production of RH neutrinos and a Dark Matter is as constrained as the thermal resonant leptogenesis. The primary restriction on the parameter space in this case comes from the branching fraction of inflaton decay to RH neutrinos and Dark matter. The branching fraction is bounded from above by $L\alpha$ constraint on Dark Matter free streaming. The maximum accessible Dark Matter mass in this scenario is approximately 320 MeV. Depending upon the inflaton mass and branching fraction, parameter spaces for Cold as well as Warm Dark Matter can also be separated. Finally, we show that in non-thermal leptogenesis scenario the Neutrino option introduces a “phantom window” in which the CP asymmetry parameter responsible for leptogenesis decreases with the increase of RH mass scale and minimally fine-tuned seesaw models naturally exhibit this phantom window.

ACKNOWLEDGEMENT

RS is supported by a Newton International Fellowship (NIF 171202). SB is supported by institute postdoctoral fellowship from Physical Research Laboratory. The authors would like to acknowledge the hospitality of WHEPP-XVI held at IIT Guwahati, INDIA, where this project was initiated.

Appendix A: Production of χ from scattering of RH neutrinos

Apart from the decay of inflaton, χ can also be produced from the scattering of RH neutrinos. In this section we have estimated the contribution of this production channel to the relic abundance of χ . Following the prescription given in [59], we can write the collision term resulting from the scatterings $N_i N_j \rightarrow \bar{\chi} \chi$ as follows

$$\mathcal{C}_{N_i N_j \rightarrow \bar{\chi} \chi} = \frac{T}{1024 \pi^6} \sum_{i,j=1}^2 \int_{(M_{N_i} + M_{N_j})^2}^{\infty} d\hat{s} \int d\Omega P_{N_i N_j} P_{\bar{\chi} \chi} |\mathcal{M}|_{N_i N_j \rightarrow \bar{\chi} \chi}^2 \frac{K_1\left(\frac{\sqrt{\hat{s}}}{T}\right)}{\sqrt{\hat{s}}}, \quad (\text{A.1})$$

where \hat{s} and $P_{\alpha\beta}$ are total energy and magnitude of 3-momentum with respect to the centre of momentum frame for initial and final states respectively. The momentum $P_{\alpha\beta}$ has the following expression

$$P_{\alpha\beta} = \frac{\sqrt{\hat{s} - (m_\alpha + m_\beta)^2} \sqrt{\hat{s} - (m_\alpha - m_\beta)^2}}{2\sqrt{\hat{s}}}, \quad (\text{A.2})$$

with m_α, m_β are the masses of particles α and β in either initial or final states. Furthermore, $d\Omega$ is the solid angle subtended by one of the outgoing particles with respect to an arbitrary direction which can be considered the direction of an incoming particle. $K_1(\frac{\sqrt{s}}{T})$ is the modified Bessel function of second kind. The Lorentz invariant matrix amplitude square for the scattering process $N_i N_j \rightarrow \bar{\chi} \chi$ is denoted by $|\mathcal{M}|_{N_i N_j \rightarrow \bar{\chi} \chi}^2$. In the present case, the expression of matrix amplitude square is given by

$$|\mathcal{M}|_{N_i N_j \rightarrow \bar{\chi} \chi}^2 = \frac{4 y_i^2 y_j^2}{(\hat{t} - m_\phi^2)^2} [(M_{\text{DM}} + M_i)^2 - \hat{t}] [(M_{\text{DM}} + M_j)^2 - \hat{t}]. \quad (\text{A.3})$$

In the above expression \hat{t} is one of the Mandelstam variables and y_i is the Yukawa coupling corresponding to the interaction $\bar{\chi} \phi N_i$. The Boltzmann equation involving the collision term $\mathcal{C}_{N_i N_j \rightarrow \bar{\chi} \chi}$ is given by,

$$\frac{dY_{\text{DM}}}{dT} = -\frac{\mathcal{C}_{N_i N_j \rightarrow \bar{\chi} \chi}}{s H T}. \quad (\text{A.4})$$

Where Y_{DM} is the comoving number density of χ and it is defined as n_{DM}/s with s being the entropy density of the universe. The Hubble parameter is indicated by H . Now, we know that $N_{\text{DM}}/Y_{\text{DM}} = \frac{\pi^4}{45} g_{*s}$, where N_χ , as defined in the Section III, is the number density of χ per N_i in ultra-relativistic thermal equilibrium. Therefore, the contribution to N_χ at the present epoch ($T = T_0$), due to the production of χ from the scatterings of RH neutrinos, is

$$N_{\text{DM}}(T_0) = -\frac{\pi^4}{45} g_{*s}(T_0) \int_{T_{\text{RH}}}^{T_0} dT \frac{\mathcal{C}_{N_i N_j \rightarrow \bar{\chi} \chi}}{s H T}, \quad (\text{A.5})$$

and T_0 being the present temperature of the universe.

Finally, the contribution of these scattering processes to the relic density of χ can be obtained from the following expression,

$$\Omega_{\text{DM}} h^2 = 3.2558 \times 10^7 \left(\frac{M_{\text{DM}}}{\text{GeV}} \right) N_{\text{DM}}(T_0). \quad (\text{A.6})$$

To estimate how much impact these scatterings have on the relic abundance of χ , we have considered a benchmark point: $m_\chi = 10^{-3}$ GeV, $M_1 = M_2 = M = 5 \times 10^6$ GeV and $m_\phi = 10^8$ GeV. For $B_\chi = 10^{-4}$, the couplings $y_1 = y_2 = y$ can be approximated as

$$y \approx \sqrt{\frac{16\pi \times 10^{-4}}{m_\phi} \left(\frac{\pi^2 g^*}{10} \right) \frac{M^2}{M_{\text{Pl}} \Phi (\sum_i K_i)^2}} \approx 10^{-9}, \quad (\text{A.7})$$

where we have taken $T_{\text{RH}} = M/\Phi (\sum_i K_i) = 2.2 \times 10^4$ GeV. Using Eqs. (A.5, A.6), we find that the contribution to $\Omega_{\text{DM}} h^2$ for this benchmark point is practically nil. This smallness is primarily due to the chosen value of $T_{\text{RH}} \ll M_i$, when the number densities of RH neutrinos are already Boltzmann suppressed. Besides, the small values of Yukawa couplings and the large inflaton mass have greatly reduced the annihilation cross section of $N_i N_j \rightarrow \bar{\chi} \chi$. Thus, we have neglected these production processes of χ in our main discussion.

[1] M. Tanabashi *et al.* [Particle Data Group], Phys. Rev. D **98**, no. 3, 030001 (2018). doi:10.1103/PhysRevD.98.030001

- [2] K. Abe *et al.* [T2K Collaboration], Phys. Rev. Lett. **118**, no. 15, 151801 (2017) doi:10.1103/PhysRevLett.118.151801 [arXiv:1701.00432 [hep-ex]].
- [3] K. Abe *et al.* [T2K Collaboration], Phys. Rev. D **96**, no. 9, 092006 (2017) Erratum: [Phys. Rev. D **98**, no. 1, 019902 (2018)] doi:10.1103/PhysRevD.96.092006, 10.1103/PhysRevD.98.019902 [arXiv:1707.01048 [hep-ex]].
- [4] K. Abe *et al.* [T2K Collaboration], Phys. Rev. Lett. **121**, no. 17, 171802 (2018) doi:10.1103/PhysRevLett.121.171802 [arXiv:1807.07891 [hep-ex]].
- [5] P. Adamson *et al.* [NOvA Collaboration], Phys. Rev. Lett. **118**, no. 23, 231801 (2017) doi:10.1103/PhysRevLett.118.231801 [arXiv:1703.03328 [hep-ex]].
- [6] M. A. Acero *et al.* [NOvA Collaboration], Phys. Rev. D **98**, 032012 (2018) doi:10.1103/PhysRevD.98.032012 [arXiv:1806.00096 [hep-ex]].
- [7] P. Adamson *et al.* [MINOS Collaboration], Phys. Rev. Lett. **110**, no. 25, 251801 (2013) doi:10.1103/PhysRevLett.110.251801 [arXiv:1304.6335 [hep-ex]].
- [8] D. Adey *et al.* [Daya Bay Collaboration], Phys. Rev. Lett. **121**, no. 24, 241805 (2018) doi:10.1103/PhysRevLett.121.241805 [arXiv:1809.02261 [hep-ex]].
- [9] G. Bak *et al.* [RENO Collaboration], Phys. Rev. Lett. **121**, no. 20, 201801 (2018) doi:10.1103/PhysRevLett.121.201801 [arXiv:1806.00248 [hep-ex]].
- [10] Y. Abe *et al.* [Double Chooz Collaboration], JHEP **1410**, 086 (2014) Erratum: [JHEP **1502**, 074 (2015)] doi:10.1007/JHEP02(2015)074, 10.1007/JHEP10(2014)086 [arXiv:1406.7763 [hep-ex]].
- [11] M. G. Aartsen *et al.* [IceCube Collaboration], Phys. Rev. D **91**, no. 7, 072004 (2015) doi:10.1103/PhysRevD.91.072004 [arXiv:1410.7227 [hep-ex]].
- [12] K. Abe *et al.* [Super-Kamiokande Collaboration], Phys. Rev. D **97**, no. 7, 072001 (2018) doi:10.1103/PhysRevD.97.072001 [arXiv:1710.09126 [hep-ex]].
- [13] I. Esteban, M. C. Gonzalez-Garcia, A. Hernandez-Cabezudo, M. Maltoni and T. Schwetz, JHEP **1901**, 106 (2019) doi:10.1007/JHEP01(2019)106 [arXiv:1811.05487 [hep-ph]].
- [14] P. Minkowski, Phys. Lett. **67B**, 421 (1977).
- [15] M. Gell-Mann, P. Ramond and R. Slansky, Conf. Proc. C **790927**, 315 (1979) [arXiv:1306.4669 [hep-th]].
- [16] T. Yanagida, Prog. Theor. Phys. **64**, 1103 (1980). R. N. Mohapatra and G. Senjanovic, Phys. Rev. Lett. **44**, 912 (1980). A variant of Type I seesaw: R. N. Mohapatra, Phys. Rev. Lett. **56**, 561 (1986).
- [17] N. Aghanim *et al.* [Planck Collaboration], Astron. Astrophys. **596**, A107 (2016) doi:10.1051/0004-6361/201628890 [arXiv:1605.02985 [astro-ph.CO]].
- [18] V. A. Kuzmin, V. A. Rubakov and M. E. Shaposhnikov, Phys. Lett. **155B**, 36 (1985). doi:10.1016/0370-2693(85)91028-7
- [19] E. W. Kolb and M. S. Turner, Front. Phys. **69**, 1 (1990).
- [20] L. Alvarez-Gaume and E. Witten, Nucl. Phys. B **234**, 269 (1984). doi:10.1016/0550-3213(84)90066-X
- [21] S. H. S. Alexander, M. E. Peskin and M. M. Sheikh-Jabbari, Phys. Rev. Lett. **96**, 081301 (2006) doi:10.1103/PhysRevLett.96.081301 [hep-th/0403069].
- [22] P. Adshead, A. J. Long and E. I. Sfakianakis, Phys. Rev. D **97**, no. 4, 043511 (2018) doi:10.1103/PhysRevD.97.043511 [arXiv:1711.04800 [hep-ph]].
- [23] J. I. McDonald and G. M. Shore, Phys. Lett. B **751**, 469 (2015) doi:10.1016/j.physletb.2015.10.075 [arXiv:1508.04119 [hep-ph]].

- [24] J. I. McDonald and G. M. Shore, JHEP **1604**, 030 (2016) doi:10.1007/JHEP04(2016)030 [arXiv:1512.02238 [hep-ph]].
- [25] A. G. Cohen and D. B. Kaplan, Phys. Lett. B **199**, 251 (1987). doi:10.1016/0370-2693(87)91369-4
- [26] H. Davoudiasl, R. Kitano, G. D. Kribs, H. Murayama and P. J. Steinhardt, Phys. Rev. Lett. **93**, 201301 (2004) doi:10.1103/PhysRevLett.93.201301 [hep-ph/0403019].
- [27] B. Feng, H. Li, M. z. Li and X. m. Zhang, Phys. Lett. B **620**, 27 (2005) doi:10.1016/j.physletb.2005.06.009 [hep-ph/0406269].
- [28] G. Lambiase and S. Mohanty, JCAP **0712**, 008 (2007) doi:10.1088/1475-7516/2007/12/008 [astro-ph/0611905].
- [29] M. Fukugita and T. Yanagida, Phys. Lett. B **174**, 45 (1986). doi:10.1016/0370-2693(86)91126-3
- [30] A. Pilaftsis and T. E. J. Underwood, Nucl. Phys. B **692**, 303 (2004) doi:10.1016/j.nuclphysb.2004.05.029 [hep-ph/0309342].
- [31] W. Buchmuller, P. Di Bari and M. Plumacher, Annals Phys. **315**, 305 (2005) doi:10.1016/j.aop.2004.02.003 [hep-ph/0401240].
- [32] S. Davidson, E. Nardi and Y. Nir, Phys. Rept. **466**, 105 (2008) doi:10.1016/j.physrep.2008.06.002 [arXiv:0802.2962 [hep-ph]].
- [33] A. Riotto and M. Trodden, Ann. Rev. Nucl. Part. Sci. **49**, 35 (1999) doi:10.1146/annurev.nucl.49.1.35
- [34] E. K. Akhmedov, V. A. Rubakov and A. Y. Smirnov, Phys. Rev. Lett. **81**, 1359 (1998) doi:10.1103/PhysRevLett.81.1359 [hep-ph/9803255].
- [35] T. Hambye and D. Teresi, Phys. Rev. Lett. **117**, no. 9, 091801 (2016) doi:10.1103/PhysRevLett.117.091801 [arXiv:1606.00017 [hep-ph]].
- [36] S. Davidson and A. Ibarra, Phys. Lett. B **535**, 25 (2002) doi:10.1016/S0370-2693(02)01735-5 [hep-ph/0202239].
- [37] F. Vissani, Phys. Rev. D **57**, 7027 (1998) doi:10.1103/PhysRevD.57.7027 [hep-ph/9709409].
- [38] G. Isidori, G. Ridolfi and A. Strumia, Nucl. Phys. B **609**, 387 (2001) doi:10.1016/S0550-3213(01)00302-9 [hep-ph/0104016].
- [39] J. D. Clarke, R. Foot and R. R. Volkas, Phys. Rev. D **91**, no. 7, 073009 (2015) doi:10.1103/PhysRevD.91.073009 [arXiv:1502.01352 [hep-ph]].
- [40] P. S. Bhupal Dev, P. Millington, A. Pilaftsis and D. Teresi, Nucl. Phys. B **886** (2014) 569 doi:10.1016/j.nuclphysb.2014.06.020 [arXiv:1404.1003 [hep-ph]].
- [41] P. S. Bhupal Dev, P. Millington, A. Pilaftsis and D. Teresi, Nucl. Phys. B **891**, 128 (2015) doi:10.1016/j.nuclphysb.2014.12.003 [arXiv:1410.6434 [hep-ph]].
- [42] I. Brivio and M. Trott, Phys. Rev. Lett. **119**, no. 14, 141801 (2017) doi:10.1103/PhysRevLett.119.141801 [arXiv:1703.10924 [hep-ph]].
- [43] I. Brivio and M. Trott, JHEP **1902**, 107 (2019) doi:10.1007/JHEP02(2019)107 [arXiv:1809.03450 [hep-ph]].
- [44] V. Brdar, Y. Emonds, A. J. Helmboldt and M. Lindner, Phys. Rev. D **99**, no. 5, 055014 (2019) doi:10.1103/PhysRevD.99.055014 [arXiv:1807.11490 [hep-ph]].
- [45] I. Brivio, K. Moffat, S. Pascoli, S. T. Petcov and J. Turner, JHEP **1910**, 059 (2019) [JHEP **2019**, 059 (2020)] doi:10.1007/JHEP10(2019)059 [arXiv:1905.12642 [hep-ph]].
- [46] V. Brdar, A. J. Helmboldt, S. Iwamoto and K. Schmitz, Phys. Rev. D **100**, 075029 (2019) doi:10.1103/PhysRevD.100.075029 [arXiv:1905.12634 [hep-ph]].

- [47] G. Bambhaniya, P. S. Bhupal Dev, S. Goswami, S. Khan and W. Rodejohann, *Phys. Rev. D* **95**, no. 9, 095016 (2017) doi:10.1103/PhysRevD.95.095016 [arXiv:1611.03827 [hep-ph]].
- [48] M. Endo, F. Takahashi and T. T. Yanagida, *Phys. Rev. D* **76**, 083509 (2007) doi:10.1103/PhysRevD.76.083509 [arXiv:0706.0986 [hep-ph]].
- [49] F. Hahn-Woernle and M. Plumacher, *Nucl. Phys. B* **806**, 68 (2009) doi:10.1016/j.nuclphysb.2008.07.032 [arXiv:0801.3972 [hep-ph]].
- [50] F. Takahashi, *Phys. Lett. B* **660**, 100 (2008) doi:10.1016/j.physletb.2007.12.048 [arXiv:0705.0579 [hep-ph]].
- [51] M. Endo, F. Takahashi and T. T. Yanagida, *Phys. Rev. D* **74**, 123523 (2006) doi:10.1103/PhysRevD.74.123523 [hep-ph/0611055].
- [52] M. Fujii, K. Hamaguchi and T. Yanagida, *Phys. Rev. D* **65**, 115012 (2002) doi:10.1103/PhysRevD.65.115012 [hep-ph/0202210].
- [53] P. S. Bhupal Dev, A. Mazumdar and S. Qutub, *Front. in Phys.* **2**, 26 (2014) doi:10.3389/fphy.2014.00026 [arXiv:1311.5297 [hep-ph]].
- [54] T. Asaka, H. B. Nielsen and Y. Takanishi, *Nucl. Phys. B* **647**, 252 (2002) doi:10.1016/S0550-3213(02)00934-3 [hep-ph/0207023].
- [55] A. Mazumdar, *Phys. Lett. B* **580**, 7 (2004) doi:10.1016/j.physletb.2003.11.032 [hep-ph/0308020].
- [56] D. Borah, S. J. Das and A. K. Saha, [arXiv:2005.11328 [hep-ph]].
- [57] R. Allahverdi, R. Brandenberger, F. Y. Cyr-Racine and A. Mazumdar, *Ann. Rev. Nucl. Part. Sci.* **60**, 27 (2010) doi:10.1146/annurev.nucl.012809.104511 [arXiv:1001.2600 [hep-th]].
- [58] E. Aprile *et al.* [XENON], *Phys. Rev. Lett.* **121**, no.11, 111302 (2018) doi:10.1103/PhysRevLett.121.111302 [arXiv:1805.12562 [astro-ph.CO]].
- [59] L. J. Hall, K. Jedamzik, J. March-Russell and S. M. West, *JHEP* **1003**, 080 (2010) doi:10.1007/JHEP03(2010)080 [arXiv:0911.1120 [hep-ph]].
- [60] A. Biswas, D. Majumdar and P. Roy, *JHEP* **04**, 065 (2015) doi:10.1007/JHEP04(2015)065 [arXiv:1501.02666 [hep-ph]].
- [61] J. König, A. Merle and M. Totzauer, *JCAP* **11**, 038 (2016) doi:10.1088/1475-7516/2016/11/038 [arXiv:1609.01289 [hep-ph]].
- [62] A. Biswas and A. Gupta, *JCAP* **09**, 044 (2016) doi:10.1088/1475-7516/2016/09/044 [arXiv:1607.01469 [hep-ph]].
- [63] A. Biswas and A. Gupta, *JCAP* **03**, 033 (2017) doi:10.1088/1475-7516/2017/03/033 [arXiv:1612.02793 [hep-ph]].
- [64] A. Biswas, D. Borah and A. Dasgupta, *Phys. Rev. D* **99**, no.1, 015033 (2019) doi:10.1103/PhysRevD.99.015033 [arXiv:1805.06903 [hep-ph]].
- [65] A. Biswas, S. Ganguly and S. Roy, *JCAP* **03**, 043 (2020) doi:10.1088/1475-7516/2020/03/043 [arXiv:1907.07973 [hep-ph]].
- [66] S. Antusch, J. Kersten, M. Lindner and M. Ratz, *Nucl. Phys. B* **674**, 401 (2003) doi:10.1016/j.nuclphysb.2003.09.050 [hep-ph/0305273].
- [67] S. Antusch, J. Kersten, M. Lindner, M. Ratz and M. A. Schmidt, *JHEP* **0503**, 024 (2005) doi:10.1088/1126-6708/2005/03/024 [hep-ph/0501272].
- [68] M. Becker, *Eur. Phys. J. C* **79**, no. 7, 611 (2019) doi:10.1140/epjc/s10052-019-7095-7 [arXiv:1806.08579 [hep-ph]].
- [69] M. Chianese and S. F. King, *JCAP* **1809**, 027 (2018) doi:10.1088/1475-7516/2018/09/027 [arXiv:1806.10606 [hep-ph]].

- [70] M. Chianese, B. Fu and S. F. King, JCAP **2003**, 030 (2020) doi:10.1088/1475-7516/2020/03/030 [arXiv:1910.12916 [hep-ph]].
- [71] P. Bandyopadhyay, E. J. Chun, R. Mandal and F. S. Queiroz, Phys. Lett. B **788**, 530 (2019) doi:10.1016/j.physletb.2018.12.003 [arXiv:1807.05122 [hep-ph]].
- [72] P. Bandyopadhyay, E. J. Chun and R. Mandal, arXiv:2005.13933 [hep-ph].
- [73] P. Di Bari, K. Farrag, R. Samanta and Y. L. Zhou, arXiv:1908.00521 [hep-ph].
- [74] N. Aghanim *et al.* [Planck], [arXiv:1807.06209 [astro-ph.CO]].
- [75] R. Samanta and M. Sen, arXiv:1908.08126 [hep-ph].
- [76] J. Hisano, K. Kohri and M. M. Nojiri, Phys. Lett. B **505**, 169 (2001) doi:10.1016/S0370-2693(01)00395-1 [hep-ph/0011216].
- [77] S. Boulebnane, J. Heeck, A. Nguyen and D. Teresi, JCAP **1804**, 006 (2018) doi:10.1088/1475-7516/2018/04/006 [arXiv:1709.07283 [hep-ph]].
- [78] M. Viel, G. D. Becker, J. S. Bolton and M. G. Haehnelt, Phys. Rev. D **88**, 043502 (2013) doi:10.1103/PhysRevD.88.043502 [arXiv:1306.2314 [astro-ph.CO]].
- [79] D. Boyanovsky, Phys. Rev. D **77**, 023528 (2008) doi:10.1103/PhysRevD.77.023528 [arXiv:0711.0470 [astro-ph]].
- [80] V. N. Senoguz and Q. Shafi, Phys. Lett. B **582**, 6 (2004) doi:10.1016/j.physletb.2003.12.020 [hep-ph/0309134].
- [81] J. A. Casas and A. Ibarra, Nucl. Phys. B **618**, 171 (2001) doi:10.1016/S0550-3213(01)00475-8 [hep-ph/0103065].
- [82] I. Esteban, M. C. Gonzalez-Garcia, M. Maltoni, I. Martinez-Soler and T. Schwetz, JHEP **1701**, 087 (2017) doi:10.1007/JHEP01(2017)087 [arXiv:1611.01514 [hep-ph]].
- [83] A. Abada, S. Davidson, A. Ibarra, F.-X. Josse-Michaux, M. Losada and A. Riotto, JHEP **0609**, 010 (2006) doi:10.1088/1126-6708/2006/09/010 [arXiv:0605281 [hep-ph]].
- [84] E. Nardi, Y. Nir, E. Roulet and J. Racker, JHEP **0601**, 164 (2006) doi:10.1088/1126-6708/2006/01/164 [arXiv:0601084 [hep-ph]].
- [85] S. Blanchet and P. Di Bari, JCAP **0703**, 018 (2007) doi:10.1088/1475-7516/2007/03/018 [hep-ph/0607330].
- [86] P. S. B. Dev, P. Di Bari, B. Garbrecht, S. Lavignac, P. Millington and D. Teresi, Int. J. Mod. Phys. A **33**, 1842001 (2018) doi:10.1142/S0217751X18420010 [arXiv:1711.02861 [hep-ph]].
- [87] R. N. Mohapatra and C. C. Nishi, JHEP **1508**, 092 (2015) doi:10.1007/JHEP08(2015)092 [arXiv:1506.06788 [hep-ph]].
- [88] R. Samanta, M. Chakraborty, P. Roy and A. Ghosal, JCAP **1703**, 025 (2017) doi:10.1088/1475-7516/2017/03/025 [arXiv:1610.10081 [hep-ph]].
- [89] R. Sinha, R. Samanta and A. Ghosal, JHEP **1712**, 030 (2017) doi:10.1007/JHEP12(2017)030 [arXiv:1706.00946 [hep-ph]].
- [90] R. Samanta, P. Roy and A. Ghosal, JHEP **1806**, 085 (2018) doi:10.1007/JHEP06(2018)085 [arXiv:1712.06555 [hep-ph]].
- [91] R. Samanta and M. Chakraborty, JCAP **1902**, 003 (2019) doi:10.1088/1475-7516/2019/02/003 [arXiv:1802.04751 [hep-ph]].
- [92] R. Samanta, R. Sinha and A. Ghosal, JHEP **1910**, 057 (2019) doi:10.1007/JHEP10(2019)057 [arXiv:1805.10031 [hep-ph]].
- [93] P. Chen, G. J. Ding and S. F. King, JHEP **1603**, 206 (2016) doi:10.1007/JHEP03(2016)206 [arXiv:1602.03873 [hep-ph]].
- [94] P. Di Bari, M. Re Fiorentin and R. Samanta, JHEP **1905**, 011 (2019) doi:10.1007/JHEP05(2019)011 [arXiv:1812.07720 [hep-ph]].

- [95] M. C. Chen and S. F. King, JHEP **0906**, 072 (2009) doi:10.1088/1126-6708/2009/06/072 [arXiv:0903.0125 [hep-ph]].
- [96] B. Dev, M. Garny, J. Klaric, P. Millington and D. Teresi, Int. J. Mod. Phys. A **33**, 1842003 (2018) doi:10.1142/S0217751X18420034 [arXiv:1711.02863 [hep-ph]].
- [97] W. Buchmuller, P. Di Bari and M. Plumacher, Nucl. Phys. B **643**, 367 (2002) Erratum: [Nucl. Phys. B **793**, 362 (2008)] doi:10.1016/S0550-3213(02)00737-X, 10.1016/j.nuclphysb.2007.11.030 [hep-ph/0205349].
- [98] V. Brdar, A. J. Helmboldt and J. Kubo, JCAP **1902**, 021 (2019) doi:10.1088/1475-7516/2019/02/021 [arXiv:1810.12306 [hep-ph]].
- [99] Y. Akrami *et al.* [Planck Collaboration], arXiv:1807.06211 [astro-ph.CO].
- [100] A. D. Linde, Phys. Rev. D **49**, 748 (1994) doi:10.1103/PhysRevD.49.748 [astro-ph/9307002].
- [101] J. Garcia-Bellido and A. D. Linde, Phys. Rev. D **57**, 6075 (1998) doi:10.1103/PhysRevD.57.6075 [hep-ph/9711360].